IOP Publishing Phys. Med. Biol. 69 (2024) 015024 https://doi.org/10.1088/1361-6560/ad120f

Physics in Medicine & Biology

IPEM Institute of Physics and Engineering in Medicine

RECEIVED
20 September 2023

REVISED
29 October 2023

ACCEPTED FOR PUBLICATION
4 December 2023

PUBLISHED
28 December 2023

PAPER

Combined BNCT-CIRT treatment planning for glioblastoma using the effect-based optimization

Yang Han[1,2], **Changran Geng**[1,*], **Saverio Altieri**[2,3], **Silva Bortolussi**[2,3], **Yuanhao Liu**[1,4], **Niklas Wahl**[5,6] and **Xiaobin Tang**[1,*]

[1] Department of Nuclear Science and Technology, Nanjing University of Aeronautics and Astronautics, Nanjing, People's Republic of China
[2] Department of Physics, University of Pavia, Pavia, Italy
[3] National Institute of Nuclear Physics, Unit of Pavia, Pavia, Italy
[4] Neuboron Medtech. Ltd, Nanjing, People's Republic of China
[5] Division of Medical Physics in Radiation Oncology, German Cancer Research Center (DKFZ), Heidelberg, Germany
[6] Institute for Radiation Oncology (HIRO) and National Center for Radiation Research in Oncology (NCRO), Heidelberg, Germany
[*] Authors to whom any correspondence should be addressed.

E-mail: gengchr@nuaa.edu.cn **and** tangxiaobin@nuaa.edu.cn

Keywords: boron neutron capture therapy, carbon ion radiotherapy, combined treatment, effect-based optimization, glioblastoma

Supplementary material for this article is available online

Abstract

Objective. Boron neutron capture therapy (BNCT) and carbon ion radiotherapy (CIRT) are emerging treatment modalities for glioblastoma. In this study, we investigated the methodology and feasibility to combine BNCT and CIRT treatments. The combined treatment plan illustrated how the synergistic utilization of BNCT's biological targeting and CIRT's intensity modulation capabilities could lead to optimized treatment outcomes. *Approach*. The Monte Carlo toolkit, TOPAS, was employed to calculate the dose distribution for BNCT, while matRad was utilized for the optimization of CIRT. The biological effect-based approach, instead of the dose-based approach, was adopted to develop the combined BNCT-CIRT treatment plans for six patients diagnosed with glioblastoma, considering the different radiosensitivity and fraction. Five optional combined treatment plans with specific BNCT effect proportions for each patient were evaluated to identify the optimal treatment that minimizes damage on normal tissue. *Main results*. Individual BNCT exhibits a significant effect gradient along with the beam direction in the large tumor, while combined BNCT-CIRT treatments can achieve uniform effect delivery within the clinical target volume (CTV) through the effect filling with reversed gradient by the CIRT part. In addition, the increasing BNCT effect proportion in combined treatments can reduce damage in the normal brain tissue near the CTV. Besides, the combined treatments effectively minimize damage to the skin compared to individual BNCT treatments. *Significance*. The initial endeavor to combine BNCT and CIRT treatment plans is achieved by the effect-based optimization. The observed advantages of the combined treatment suggest its potential applicability for tumors characterized by pleomorphic, infiltrative, radioresistant and voluminous features.

1. Introduction

Boron neutron capture therapy (BNCT) is a cancer-selective radiotherapy modality commonly employed in the treatment of glioblastoma, melanoma, and head and neck cancer (Dymova *et al* 2020). The therapeutic dose of BNCT is mainly attributed to the nuclear reaction between externally irradiated neutrons and tumor-enriched ^{10}B drugs, producing alpha and lithium particles with a short range that selectively damage tumor cells while sparing surrounding normal cells (Barth *et al* 2018). In addition, BNCT has a high relative biological effectiveness (RBE) and is often applied in cases of recurrence following conventional radiotherapy. However, the issue of non-uniform dose distribution within tumors has consistently posed a challenge in the context of

BNCT (Yu *et al* 2017). Multi-field neutron beams have the potential to enhance the dose distribution to large tumors (Fujimoto *et al* 2015, Lee *et al* 2017), which is similar to the principle of three-dimensional conformal radiotherapy (3D CRT). However, neutron beams are difficult to achieve intensity modulation within a single field considering its forward angle and field size. Clinical investigations into BNCT employing multiple fields have also been undertaken at institutions such as Harvard-MIT (Palmer *et al* 2002, Busse *et al* 2003). Nonetheless, the limited penetration capacity of neutron has made it challenging to formulate BNCT treatment plans that incorporate multiple fields covering a full range of angles.

Carbon ion radiotherapy (CIRT) is a therapeutic modality that relies on the Bragg peak of carbon ions to achieve a precise and conformal dose deposition in tumors (Durante and Paganetti 2016). Furthermore, CIRT has high RBE values, comparable to that of BNCT, enabling the efficient destruction of radiation-resistant tumors (Karger and Peschke 2017). Nevertheless, due to the steep dose gradient at the tumor periphery, accurate tumor identification and contouring, precise positioning, and meticulous beam control are crucial (Paganetti 2012, Han *et al* 2019, Geng *et al* 2020).

In recent years, the simultaneous implementation of different treatment modalities in radiotherapy has gained increasing attention to improving treatment efficacy, although such approaches have yet to be widely adopted in clinical practice. Several combined regimens have been proposed, including electron–photon (Renaud *et al* 2019), proton–photon (Unkelbach *et al* 2018, Gao 2019, Fabiano *et al* 2020, Marc *et al* 2021, Li *et al* 2023), carbon-photon (Bennan *et al* 2021), and BNCT-photon/proton modality (Takada *et al* 2020). In this study, we aimed to evaluate the feasibility and potential benefits of combining BNCT and CIRT. We hypothesize that the combined BNCT-CIRT modality has the potential to provide a more homogeneous dose distribution to the tumor and reduce the normal tissue toxicity by combining the BNCT's biological targeting and CIRT's intensity modulation capabilities. To explore this hypothesis, we conducted the initial endeavor of the combined BNCT-CIRT treatment planning using the effect-based optimization for patients diagnosed with glioblastoma.

2. Methods and materials

2.1. Software

The BNCT dose calculation was accomplished using the Monte Carlo simulation software TOPAS 3.7, known for its high accuracy and reliability (Perl *et al* 2012, Faddegon *et al* 2020). The modular physics list included 'g4em-standard_opt4', 'thermalphp_physics', 'g4decay', 'g4ion-binarycascade', 'g4h-elastic_HP', 'g4stopping', and 'g4em-extra' (Zhang *et al* 2019). Additionally, the CIRT optimization was performed using matRad v2.10.1, an open-source radiation treatment planning system (Wieser *et al* 2017).

2.2. Sources

In this study, the 'Neuboron source', an accelerate-based neutron beam constructed by Neuboron Medtech. Ltd., was utilized. This neutron beam was generated through the reaction between 2.5 MeV protons and a lithium target with 93.1 mm thickness (Lee *et al* 2014). The carbon ion beam employed in this study was provided by the 'Generic' beam model included in matRad.

2.3. Patients

In this investigation, the efficacies of the BNCT, CIRT, and combined BNCT-CIRT treatment strategy were assessed for six patients diagnosed with glioblastoma. All cases were obtained from the database of Jiangsu Cancer Hospital, with patients' consent to use their data anonymously for research purposes. Experienced radiation oncologists performed the delineation of the clinical target volume (CTV). The brain and skin were identified as organs at risk. Conversion of CT-HU values to corresponding materials was conducted using the method proposed by Schneider *et al* for Monte Carlo simulation (Schneider *et al* 2000). The dose calculation matrix in TOPAS and matRad preserved the original CT resolution.

2.4. Effect-based optimization

Considering the nonlinear effects stemming from fractionation and the variable RBE values of CIRT and BNCT, this study utilized the biological effect ε, which represents the negative logarithm of the surviving fraction S, for the joint optimization of combined BNCT-CIRT treatment plans (Wilkens and Oelfke 2004, Wilkens and Oelfke 2006):

$$\varepsilon = -\log(S) = \alpha d + \beta d^2. \tag{1}$$

The application of the biological effect ε in the optimization process is rooted in the Linear-Quadratic (LQ) model, which is a widely accepted framework for guiding fractionation decisions in radiobiology. The

Table 1. Parameter values in different volumes for biological weighted dose and effect calculation in BNCT.

i		Q_i (ppm)	W_i^{boron}	W_i^{fn}	W_i^{tn}	W_i^{γ}	α_i^{γ} (Gy^{-1})	β_i^{γ} (Gy^{-2})
$i \in$ CTV	—	60	3.5	3.2	3.2	1	0.5	0.05
$i \notin$ CTV	$i \in$ Skin	25	2.5	3.2	3.2	1	0.1	0.05
	$i \notin$ Skin	18	1.4	3.2	3.2	1	0.1	0.05

parameters α and β are used to characterize the radiation sensitivity. This effect-based optimization approach has been successfully implemented in the planning of CIRT and IMRT-CIRT treatments (Bennan *et al* 2021).

In the case of the combined BNCT-CIRT treatment, where the number of fractions for CIRT (n^{CIRT}) is predetermined and BNCT is administered in a single fraction (i.e. $n^{BNCT} = 1$) in this study, the optimization problem can be expressed as follows:

$$\min_{x_k} \sum_m w_m f_m(\varepsilon^{Total}) \tag{2}$$

$$\varepsilon_i^{Total} = n^{CIRT}\varepsilon_i^{CIRT} + n^{BNCT}\varepsilon_i^{BNCT} \quad \forall\, i \tag{3}$$

in which $f_m(\varepsilon^{Total})$ and w_m are the objective functions and associated penalties for different structures (m), evaluated for the cumulative biological effect ε^{Total} of BNCT and CIRT fractions combined in voxel i, x_k is the intensity of carbon ion pencil beam k. The biological effect of a single CIRT fraction (ε_i^{CIRT}) is represented as follows:

$$\varepsilon_i^{CIRT} = \sum_k \alpha_{i,k}^{CIRT} D_{i,k}^{CIRT} x_k + \left(\sum_k \sqrt{\beta_{i,k}^{CIRT}} D_{i,k}^{CIRT} x_k\right)^2 \quad \forall\, i \tag{4}$$

in which $D_{i,k}^{CIRT}$ denotes its absorbed dose contribution to voxel i for unit beam intensity, $\alpha_{i,k}^{CIRT}$ and $\beta_{i,k}^{CIRT}$ are calculated based on the local effect model IV (LEM IV) (Grün *et al* 2012). The biological effect of BNCT (ε_i^{BCNT}) is calculated by equation (5):

$$\varepsilon_i^{BNCT} = \alpha_i^{\gamma} d_i^{BNCT} + \beta_i^{\gamma} (d_i^{BNCT})^2 \quad \forall\, i \tag{5}$$

in which α_i^{γ} and β_i^{γ} are the LQ model parameters of photon, d_i^{BNCT} is the biological weighted dose of BNCT (i.e. photon equivalent dose). This differs from the CIRT approach in equation (4), as radiosensitivity is not modeled through BNCT-specific α and β parameters. Instead, according to different relative biological effectiveness (W) and absorbed dose per ppm of boron (D) of each dose component, the biological weighted dose of BNCT can be described by equation (6):

$$d_i^{BNCT} = Q_i W_i^{boron} D_i^{boron} + W_i^{fn} D_i^{fn} + W_i^{tn} D_i^{tn} + W_i^{\gamma} D_i^{\gamma} \quad \forall\, i \tag{6}$$

in which Q is the boron concentration, D with superscripts boron, fn, tn, and γ represent boron dose, fast neutron dose, thermal neutron dose, and gamma dose, respectively. All the fixed parameters required for the calculation of the biological weighted dose and effect in BNCT (Yu *et al* 2017, Bennan *et al* 2021) were presented in table 1.

2.5. Treatment planning study

The Flow chart of combined treatment planning optimization is depicted in figure 1. The combined treatment plan can be split into two parts: the BNCT part and the CIRT part. In the BNCT part, a 'Neuboron source' with a radius of 10 cm was employed, and irradiation was administered from the top of the patient's head. In the CIRT part, two coplanar carbon beams were utilized, and the number of fractions was set to 30 (i.e. $n^{CIRT} = 30$). The number of treatment fractions was fixed to minimize variation in this study, but it can be optimized in actual treatment. A Monte Carlo simulation was performed to obtain the effect distribution matrix of BNCT. To assess the impact of the BNCT effect proportion and determine an optimal ratio of BNCT and CIRT in the combined treatment modality, we adjusted the effect matrix of the BNCT part to attain a desired value of $\varepsilon_{CTV95\%}^{BNCT}$ in the CTV. In this study, we set $\varepsilon_{CTV95\%}^{BNCT}$ to 1.8, 3.6, 5.4, 7.2, and 9, corresponding to 5%, 10%, 15%, 20%, and 25% of the prescription effect limit. The relative combined treatments are labeled as Hybrid_1, Hybrid_2, Hybrid_3, Hybrid_4, and Hybrid_5, respectively. Then, the effect matrix of the BNCT part was used as a fixed base matrix for CIRT optimization. To aid comparability, we scaled all combined plans to the same target coverage (i.e. 95% of the biological effect reaching the CTV).

The accumulated treatment quality metric is expressed in the form of 2 Gy equivalent dose ($EQD2$), a more common parameter in clinical plan analysis. The relationship between $EQD2_i$ and ε_i^{Total} is shown in

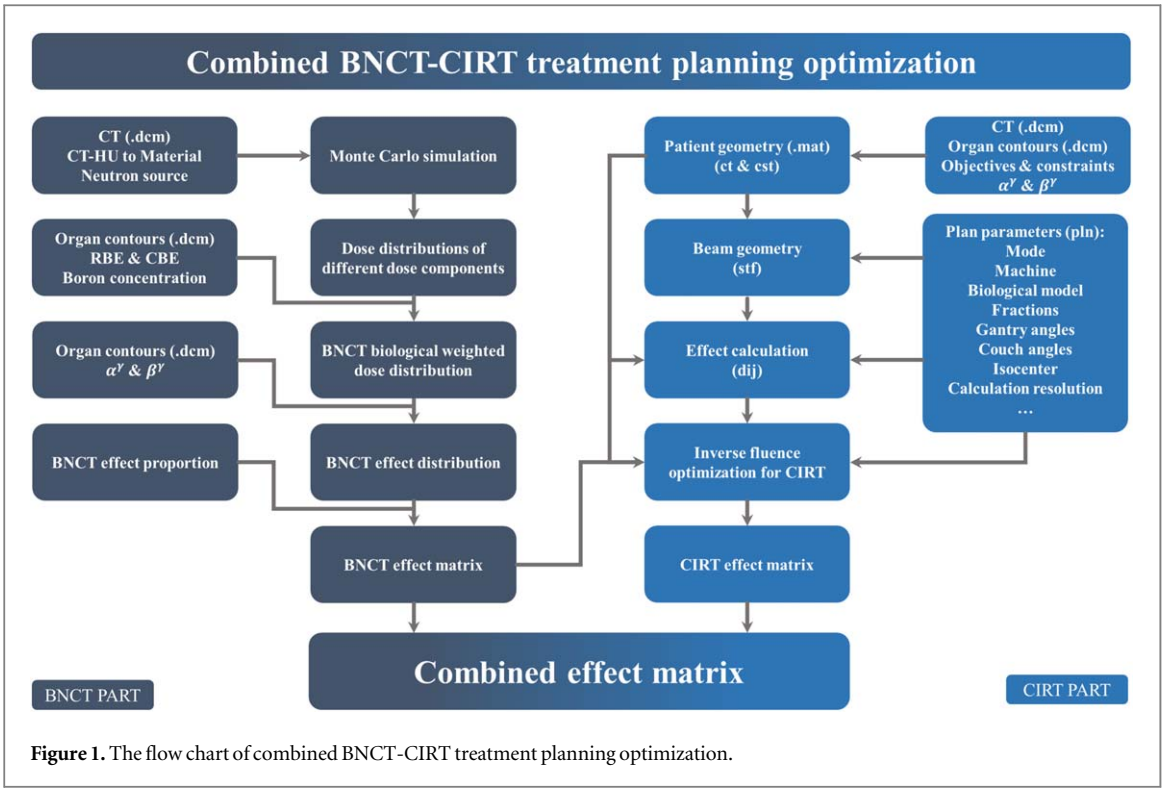

Figure 1. The flow chart of combined BNCT-CIRT treatment planning optimization.

equation (7).

$$EQD2_i = \frac{\varepsilon_i^{\mathrm{Total}} / \alpha_i^{\gamma}}{1 + 2 / (\alpha_i^{\gamma} / \beta_i^{\gamma})} \quad \forall\, i. \tag{7}$$

In this study, we adopted a reference treatment standard for glioblastoma with photon radiotherapy delivered at a dose of 2 Gy/30 fractions, and the maximum dose limit for normal brain tissue was set to 60 Gy (Emami 2013, Gzell *et al* 2017). According to equation (7), the prescription effect limit in the CTV was 36 ($\alpha^{\gamma}/\beta^{\gamma} = 0.5/0.05$ Gy), while the maximum allowable effect limit in normal brain tissue was determined to be 12 ($\alpha^{\gamma}/\beta^{\gamma} = 0.1/0.05$ Gy). Specifically, we used the optimization function 'Squared Deviation' within matRad, setting ε in the CTV to 36 with a penalty value of 50, and the 'Squared Overdosing' function for normal brain tissue with an ε of 12 and a penalty value of 500. The detailed explanation of these optimization parameters and the exact definition of the function in matRad can be found in the published paper (Wieser *et al* 2017) or in the open-source code repository (http://github.com/e0404/matRad/tree/v2.10.1).

3. Results

Figure 2 displays the cumulative effect distributions in the treatment plans for patient 1 as an example when using individual BNCT or CIRT. The figure comprises three slices (i.e. sagittal, coronal, and axial) for each treatment approach. Upon analyzing figures 2(a)–(b), a noticeable effect gradient in the CTV along the beam direction is observed when utilizing BNCT alone (i.e. the cumulative effect is higher when the voxel is close to the top of the head and lower at depth). This outcome arises due to the decreased beam flux during neutron transport into the patient. To ensure that 95% of the CTV attains the prescribed effect limit (i.e. $\varepsilon_{\mathrm{CTV95\%}}^{\mathrm{BNCT}} = 36$), the maximum effect in the CTV reaches 250. Figure 1(c) presents the effect distribution in the vertical plane of the beam, which facilitates the characteristic of BNCT to spare the normal brain tissue depending on its biological targeting property. Conversely, figures 2(d)–(f) demonstrate that CIRT can achieve a uniform distribution of the cumulative effect in the CTV through intensity modulation, but normal brain tissue near CTV would have a higher cumulative effect considering the gradient of the spread-out Bragg peak.

Figure 3 depicts the cumulative effect distributions in the treatment plans for patient 1 when the combined BNCT-CIRT modality (i.e. a single fraction of BNCT and thirty fractions of CIRT) is utilized. The figure displays a single slice direction to visualize the effect change tendency along the neutron beam. The results for five different combined treatments (Hybrid_1~Hybrid_5) are shown in separated columns. The BNCT part, CIRT part, and BNCT+CIRT effect distributions of the combined treatments are presented in different rows. Figures 3(a)–(e) reveals a gradient of effect distribution along the beam direction in the BNCT part, while figures 3(f)–(j) show how CIRT compensates for this gradient to achieve a uniform effect distribution in the CTV

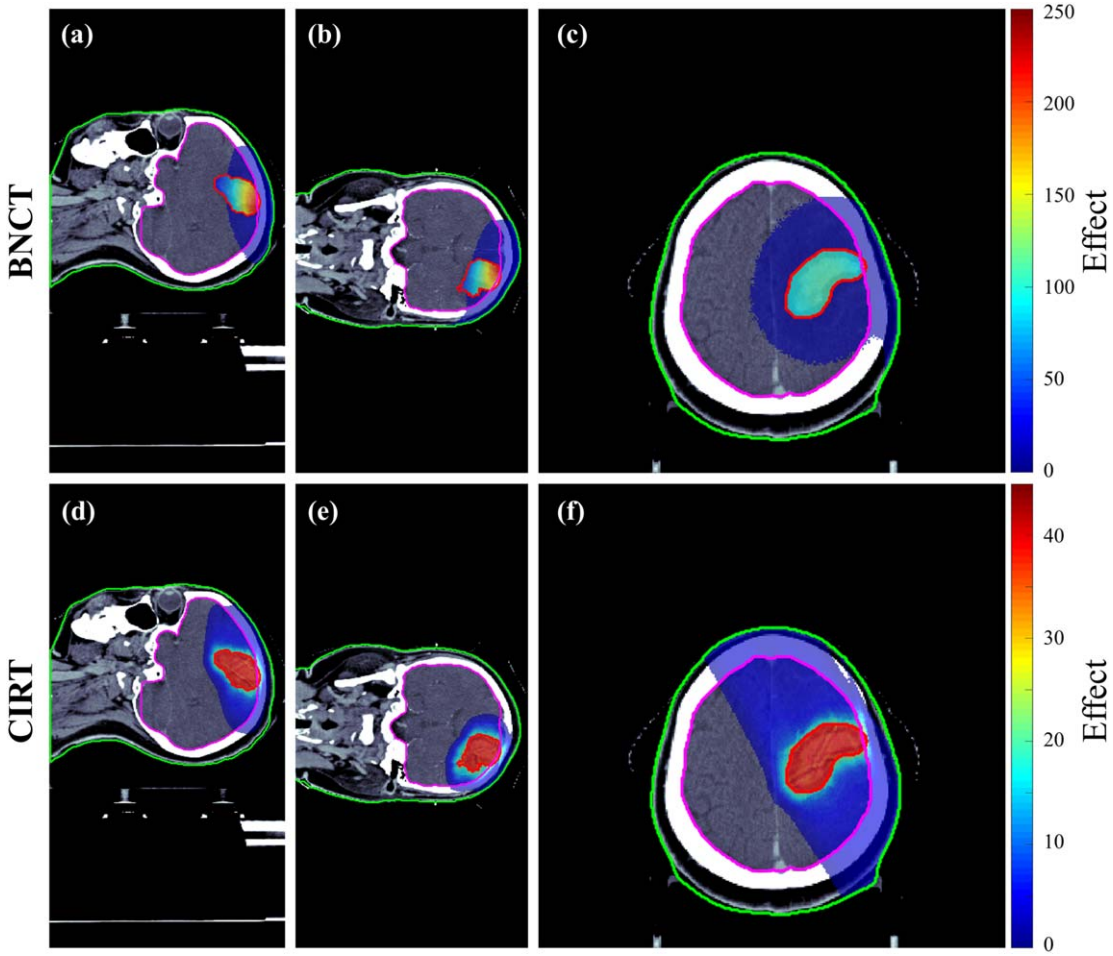

Figure 2. The cumulative effect distributions in the treatment plans for patient 1 when using individual BNCT (a)–(c) or CIRT (d)–(f). Three slices are presented for each treatment approach, i.e. sagittal: (a) and (d), coronal: (b) and (e), axial: (c) and (f). Organ contours are delineated using lines of different colors: CTV (red), brain (pink), and skin (green).

for each combined treatment, as shown in figures 3(k)–(o). Specifically, the CIRT beam fluences are optimized to give an inverse gradient of effect distribution within the CTV.

Figure 4 presents the effect volume histograms (EVHs) of combined treatment plans for patient 1 when the combined BNCT-CIRT modality (i.e. a single fraction of BNCT and thirty fractions of CIRT) is utilized. Distinct color schemes are employed to represent the combined treatment plans, each corresponding to specific effect proportions attributed to BNCT. In figure 4(c), the combined treatment, Hybrid_5, exhibits a trailing high-effect area due to excessive BNCT effect in the voxels near the top of the head. Apart from this, the homogeneity of effect in the CTV has little variation among different combined treatments. Figure 4(f) illustrates that as the proportion of BNCT effect increases (i.e. from Hybrid_1 to Hybrid_5), less normal brain tissue is exposed to high effects. Furthermore, by analyzing the figure 4(i), we found no significant pattern in skin exposure for different combined treatments. Supplementary A presents the effect volume histograms of combined treatments for patient 2 to patient 6.

Figure 5 displays the EVHs of individual BNCT, CIRT, and the artificially selected (optimized) combined treatments from Hybrid_1 to Hybrid_5 for six patients. Table 2 lists the relevant EQD2-based quality indicator values of BNCT, CIRT, and the selected combined treatment for each patient. For patients 1–4, the combined treatments exhibit advantages when the same prescribed dose/effect is reached within the CTV. Specifically, the combined treatment presents superior dose/effect delivery in the CTV and skin in comparison to BNCT, while it gives improved dose/effect delivery in the normal brain tissue compared to CIRT. Nevertheless, the combined BNCT-CIRT treatment also has some limitations for the other two cases. For patient 5, all three treatment approaches (i.e. BNCT, CIRT, and Hybrid_5) can achieve satisfactory results because of the small volume and superficial location of the tumor, for which the combined treatment has no significant advantages. For patient 6, although the combined treatment (i.e. Hybrid_1) shows some improvement, it still poses a high risk of side effects in the normal tissue because of the deep tumor location. Supplementary B gives the complete EQD2-based quality indicator values including other combined treatments for each patient.

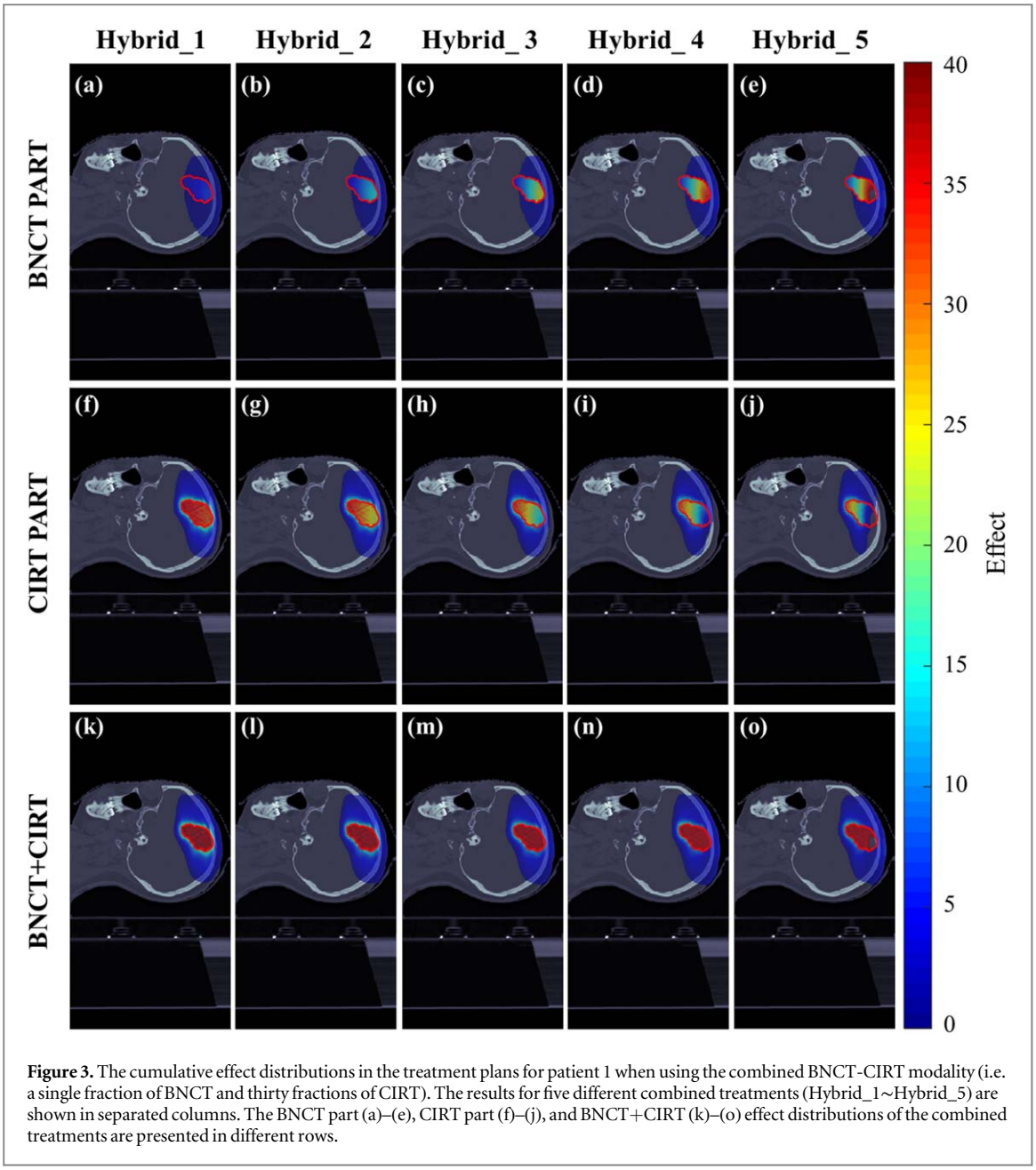

Figure 3. The cumulative effect distributions in the treatment plans for patient 1 when using the combined BNCT-CIRT modality (i.e. a single fraction of BNCT and thirty fractions of CIRT). The results for five different combined treatments (Hybrid_1∼Hybrid_5) are shown in separated columns. The BNCT part (a)–(e), CIRT part (f)–(j), and BNCT+CIRT (k)–(o) effect distributions of the combined treatments are presented in different rows.

4. Discussion

This study employed an effect-based optimization approach to develop the combined BNCT-CIRT treatment plan. The feasibility and advantages of the combined treatment modality were assessed by comparing the cumulative effect distributions and EVHs of individual BNCT, CIRT, and the combined treatment. Specifically, for BNCT, the significant effect gradient in large tumors always results in unacceptable damage to superficial normal tissue (e.g. skin) when attempting to achieve the prescribed dose/effect in the large CTV. In conventional radiotherapy, this can be solved by multiple fields and varying fluences, but it is still a challenge in BNCT, considering the limitation on neutron beam and boron drugs delivery (Yu *et al* 2017). Therefore, combining BNCT with other intensity-modulated radiotherapies, which can achieve the effect filling with reversed gradient, may have potential solve the problem. Moreover, the reason for selecting the combined BNCT-CIRT modality is that both treatment modalities predominantly utilize heavy ions with high RBE values, which may be more in line with the clinical interest to treat cancers with high radioresistant (Reya *et al* 2001, Tsujii *et al* 2004). Nevertheless, the effect-based optimization approach employed in this study is not exclusive to the combination of BNCT with CIRT but can also be used in BNCT-photon, BNCT-proton, or other BNCT-ion combinations, as it in general allows any combination of modalities that can formulate response in the LQ framework. Furthermore, we found that the increasing effect proportion of BNCT in the combined treatments can reduce damage to the normal brain tissue, particularly in close proximity to the CTV. This is attributed to

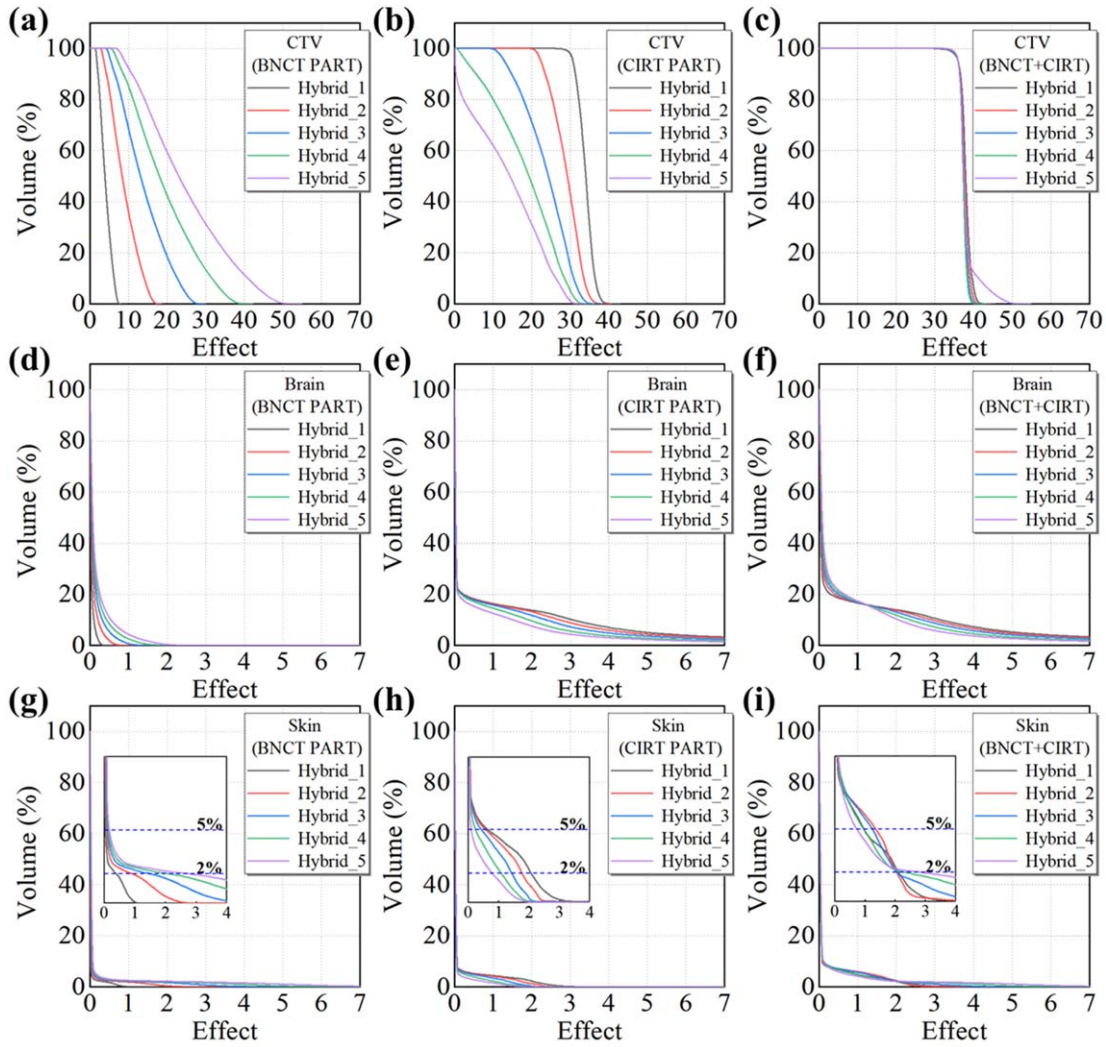

Figure 4. The effect volume histograms of combined treatment plans for patient 1 when using the combined BNCT-CIRT modality (i.e. a single fraction of BNCT and thirty fractions of CIRT). Five different combined treatments are depicted in distinct colors: Hybrid_1 (black), Hybrid_2 (red), Hybrid_3 (blue), Hybrid_4 (green), and Hybrid_5 (purple). Different rows corresponding to results for three organ contours: CTV (a)–(c), Brain (d)–(f), Skin (g)–(i); separated columns represent the BNCT part (a), (d), (g), CIRT part (b), (e), (h), and BNCT+CIRT (c), (f), (i) in the combined treatments. Subplots in figures (g)–(i) provide magnified EVHs with auxiliary lines representing the 5% and 2% volumes.

the biological targeting property of BNCT. These findings highlight the potential of combined BNCT-CIRT modality to achieve optimal tumor control while minimizing normal tissue toxicity.

Tumor volume and location appear to be a necessary consideration for combined BNCT-CIRT treatment. For small superficial tumors (e.g. patient 5), individual BNCT and CIRT can achieve satisfactory results, and the combined modality has few significant advantages. Besides, for tumors located deeply (e.g. patient 6), the combined BNCT-CIRT treatment may not achieve acceptable results due to the high cost of delivering dose/effect into the deep CTV using the BNCT approach. Multi-field CIRT may be a more suitable choice in such cases (Lautenschlaeger *et al* 2022).

When considering the combination of BNCT and CIRT, both high RBE therapies, its applicability may extend to scenarios involving recurrent tumors that have acquired radioresistant following the initial treatment. To illustrate, patients diagnosed with recurrence glioblastoma may have undergone a course of treatment consisting of 60 Gy of x-ray radiotherapy combined with temozolomide (Chamberlain *et al* 2007). In such instances, challenges persist to determine the prescribed dose and assess the toxicity on normal tissues.

Heterogeneity in macroscopic and microscopic boron distribution can affect the dose or effect calculation in BNCT, and may also impact the efficacy of the combined BNCT-CIRT treatment. The inhomogeneous macroscopic boron distribution in the same organ stems from differences in tissue environment (e.g. microvessel density) (Aihara *et al* 2006). This macroscopic heterogeneity can lead to significant localized effect gradients. Quantitative measurements of macroscopic boron distribution can be achieved by PET imaging or prompt gamma imaging (Teng *et al* 2023, Wu *et al* 2023). However, the challenge is to recognize if CIRT could

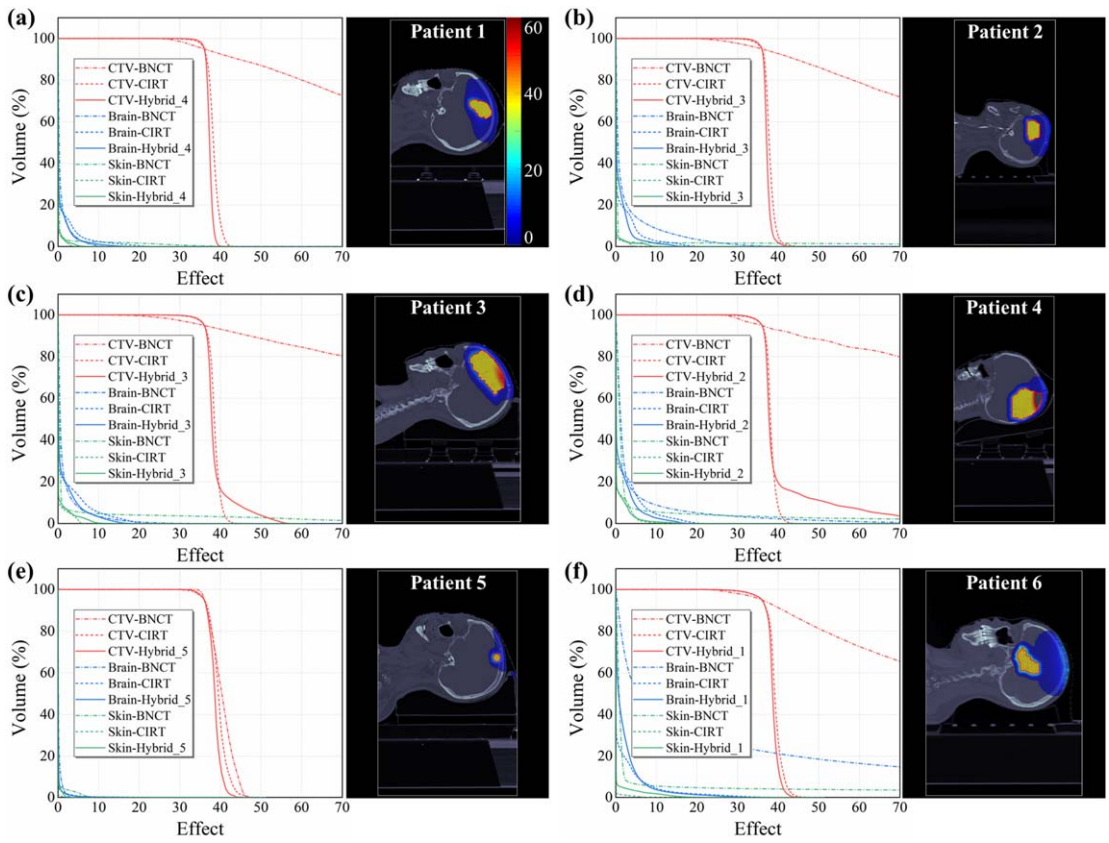

Figure 5. The effect volume histograms of individual BNCT (dash-dotted line), CIRT (dashed line), and the artificially selected (optimized) combined treatment (solid line) from Hybrid_1 to Hybrid_5 for six patients. The relevant CT slice and cumulative effect distribution of the selected combined treatment for each patient are shown in the corresponding plot.

Table 2. EQD2-based quality indicators of BNCT, CIRT and the selected combined treatments for six patients.

EQD2-based quality indicators (Unit: Gy)		Patient 1			Patient 2			Patient 3		
		CTV 35.12 cm^3			CTV 67.87 cm^3			CTV 137.97 cm^3		
		BNCT	CIRT	Hybrid_4	BNCT	CIRT	Hybrid_3	BNCT	CIRT	Hybrid_3
CTV	$D_{95\%}$	60.00	60.00	60.00	60.00	59.98	60.00	60.00	60.02	60.00
	D_{max}	421.00	75.07	68.33	646.82	79.18	71.77	919.65	79.53	96.95
	D_{mean}	186.47	63.82	62.15	219.40	63.10	62.07	314.85	64.10	64.97
Brain	$D_{5\%}$	20.85	27.85	19.10	81.30	32.80	21.40	37.75	52.65	38.10
	$D_{2\%}$	33.40	57.65	35.50	122.75	63.45	43.75	68.70	80.80	59.55
Skin	$D_{5\%}$	2.75	3.55	4.75	2.15	0.15	2.00	38.50	14.30	15.95
	$D_{2\%}$	69.00	11.70	11.55	22.45	14.30	15.00	304.95	24.05	35.85
EQD2-based quality indicators (Unit: Gy)		Patient 4			Patient 5			Patient 6		
		CTV 127.88 cm^3			CTV 1.87 cm^3			CTV 31.43 cm^3		
		BNCT	CIRT	Hybrid_2	BNCT	CIRT	Hybrid_5	BNCT	CIRT	Hybrid_1
CTV	$D_{95\%}$	60.00	60.03	60.02	60.00	59.97	60.02	60.00	59.98	59.98
	D_{max}	2590.4	75.40	146.83	77.85	81.08	75.97	1238.4	81.38	76.53
	D_{mean}	559.77	63.58	68.47	67.33	65.85	64.28	251.88	65.25	64.33
Brain	$D_{5\%}$	101.95	46.85	34.80	5.85	0.50	2.20	929.20	46.10	41.85
	$D_{2\%}$	215.75	77.30	58.00	9.10	9.00	8.15	1377.2	87.10	77.15
Skin	$D_{5\%}$	68.85	20.45	18.05	3.35	0.00	1.25	76.75	0.00	6.85
	$D_{2\%}$	383.05	27.00	29.45	26.20	0.00	6.10	2450.5	0.80	44.30

effectively address the significant effect gradient through intensity modulation considering the limitation of beam delivering, and whether the combined therapy could still demonstrate its advantages under more complex conditions. In addition, the heterogeneous microscopic boron distribution due to distinct drug transport mechanisms is a crucial factor which did not consider in the present study. Given the limited range of alpha and lithium particles resulting from the boron neutron capture reaction, the microscopic distribution significantly influences the W_i^{boron} value in BNCT (Sato *et al* 2018, Han *et al* 2023). It is noteworthy that although this study employed an effect-based approach, challenges persisted in obtaining BNCT-specific α and β data. Accordingly, the effect calculation in this study amalgamated the RBE-weighted (e.g. W_i^{boron}) dose with the α and β data of photons. Nevertheless, the microscopic heterogeneity in boron distribution can also influence BNCT-specific α and β data. Considering the effect of heterogeneous microscopic boron distribution, the CIRT part in combined treatment may still achieve reversed effect distribution through intensity modulation in theory because the effect gradient in the BNCT part induced by the microscopic boron distribution is relatively small.

Furthermore, there are some limitations and prospects for the treatment planning process in this study. Fractionation optimization merits consideration for certain patients, such as combining a single fraction of BNCT with a single fraction of CIRT. Although the LQ model is extensively utilized in radiation therapy to assess the impact of radiation on tumors and normal tissue, it possesses inherent limitations in comprehensively capturing the intricate biological response. The LQ model does not account for crucial factors, including the dynamic immune system response, intercellular interactions, and anatomical structural changes, which have substantial implications on treatment outcomes. (Sharma and Allison 2015, Brock *et al* 2017). Besides, the accuracy of the biological effect calculation is highly dependent on the α and β values. The study conducted by Fertil *et al* highlighted the heterogeneity of α and β values across different normal and tumor tissue (Fertil and Malaise 1985). These values, which reflect the intrinsic radiosensitivity and repair capacity, were acknowledged in this study but simplified for practical considerations. Future investigations that incorporate these variations are necessary to optimize treatment strategies.

5. Conclusions

This study presented the initial endeavor to combine BNCT and CIRT treatment using the effect-based optimization approach, aiming to assess its potential advantages by comparing the outcomes with those of individual BNCT and CIRT treatments. The findings from the analysis of six patients diagnosed with glioblastoma highlight the benefits of the combined treatment strategy, including the achievement of a more homogeneous effect distribution within the CTV and the reduction of dose/effect delivery to the skin and normal brain tissue, though this modality is not suitable for deeply located tumors. The observed advantages of the combined BNCT-CIRT treatment suggest its potential applicability for tumors characterized by pleomorphic, infiltrative, radioresistant, and voluminous features.

Acknowledgments

This work was supported by the National Natural Science Foundation of China (Grant No. 12261131621); the National Key Research and Development Program (Grant No. 2022YFE0107800); the Natural Science Foundation of Jiangsu Province (Grant No. BK20220132); the Deutsche Forschungsgemeinschaft (Grant No. 443188743).

Data availability statement

All data that support the findings of this study are included within the article (and any supplementary information files).

ORCID iDs

Changran Geng https://orcid.org/0000-0002-6332-6193
Saverio Altieri https://orcid.org/0000-0002-1376-3686
Silva Bortolussi https://orcid.org/0000-0003-0452-2255
Niklas Wahl https://orcid.org/0000-0002-1451-223X
Xiaobin Tang https://orcid.org/0000-0003-3308-0468

References

Aihara T, Hiratsuka J, Morita N, Uno M, Sakurai Y, Maruhashi A, Ono K and Harada T 2006 First clinical case of boron neutron capture therapy for head and neck malignancies using F-18-BPA pet *Head Neck-J. Sci. Specialties Head Neck* **28** 850–5

Barth R F, Zhang Z and Liu T 2018 A realistic appraisal of boron neutron capture therapy as a cancer treatment modality *Cancer Commun.* **38** 1–7

Bennan A B, Unkelbach J, Wahl N, Salome P and Bangert M 2021 Joint optimization of photon-carbon ion treatments for glioblastoma *Int. J. Radiat. Oncol. Biol. Phys.* **111** 559–72

Brock K K, Mutic S, McNutt T R, Li H and Kessler M L 2017 Use of image registration and fusion algorithms and techniques in radiotherapy: report of the AAPM radiation therapy committee task *Med. Phys.* **44** E43–76

Busse P M, Harling O K, Palmer M R, Kiger W, Kaplan J, Kaplan I, Chuang C F, Tim Goorley J, Riley K J and Newton T H 2003 A critical examination of the results from the Harvard-MIT NCT program phase I clinical trial of neutron capture therapy for intracranial disease *J. Neuro-Oncol.* **62** 111–21

Chamberlain M C, Glantz M J, Chalmers L, Van Horn A and Sloan A E 2007 Early necrosis following concurrent Temodar and radiotherapy in patients with glioblastoma *J. Neuro-Oncol.* **82** 81–3

Durante M and Paganetti H 2016 Nuclear physics in particle therapy: a review *Rep. Prog. Phys.* **79** 096702

Dymova M A, Taskaev S Y, Richter V A and Kuligina E V 2020 Boron neutron capture therapy: current status and future perspectives *Cancer Commun.* **40** 406–21

Emami B 2013 Tolerance of normal tissue to therapeutic radiation *Rep. Radiother. Oncol.* **1** 123–7 https://brieflands.com/articles/rro-2782

Fabiano S, Balermpas P, Guckenberger M and Unkelbach J 2020 Combined proton–photon treatments—a new approach to proton therapy without a gantry *Radiother. Oncol.* **145** 81–7

Faddegon B, Ramos-Méndez J, Schuemann J, McNamara A, Shin J, Perl J and Paganetti H 2020 The TOPAS tool for particle simulation, a Monte Carlo simulation tool for physics, biology and clinical research *Phys. Med.* **72** 114–21

Fertil B and Malaise E P 1985 Intrinsic radiosensitivity of human cell lines is correlated with radioresponsiveness of human tumors: analysis of 101 published survival curves *Int. J. Radiat. Oncol. Biol. Phys.* **11** 1699–707

Fujimoto N, Tanaka H, Sakurai Y, Takata T, Kondo N, Narabayashi M, Nakagawa Y, Watanabe T, Kinashi Y and Masunaga S 2015 Improvement of depth dose distribution using multiple-field irradiation in boron neutron capture therapy *Appl. Radiat. Isot.* **106** 134–8

Gao H 2019 Hybrid proton–photon inverse optimization with uniformity-regularized proton and photon target dose *Phys. Med. Biol.* **64** 105003

Geng C, Han Y, Tang X, Shu D, Gong C and Altieri S 2020 Evaluation of using the Doppler shift effect of prompt gamma for measuring the carbon ion range *in vivo* for heterogeneous phantoms *Nucl. Instrum. Methods Phys. Res.*A **959** 163439

Grün R, Friedrich T, Elsässer T, Krämer M, Zink K, Karger C, Durante M, Engenhart-Cabillic R and Scholz M 2012 Impact of enhancements in the local effect model (LEM) on the predicted RBE-weighted target dose distribution in carbon ion therapy *Phys. Med. Biol.* **57** 7261

Gzell C, Back M, Wheeler H, Bailey D and Foote M 2017 Radiotherapy in glioblastoma: the past, the present and the future *Clin. Oncol.* **29** 15–25

Han Y, Geng C, Liu Y, Wu R, Li M, Yu C, Altieri S and Tang X 2023 Calculation of the DNA damage yield and relative biological effectiveness in boron neutron capture therapy via the Monte Carlo track structure simulation *Phys. Med. Biol.* **68** 175028

Han Y, Tang X, Geng C, Shu D, Gong C, Zhang X, Wu S and Zhang X 2019 Investigation of *in vivo* beam range verification in carbon ion therapy using the doppler shift effect of prompt gamma: a monte Carlo simulation study *Radiat. Phys. Chem.* **162** 72–81

Karger C P and Peschke P 2017 RBE and related modeling in carbon-ion therapy *Phys. Med. Biol.* **63** 01TR02

Lautenschlaeger F S, Dumke R, Schymalla M, Hauswald H, Carl B, Stein M, Keber U, Jensen A, Engenhart-Cabillic R and Eberle F 2022 Comparison of carbon ion and photon reirradiation for recurrent glioblastoma *Strahlentherapie Und Onkologie* **198** 427–35

Lee J-C, Chuang K-S, Chen Y-W, Hsu F-Y, Chou F-I, Yen S-H and Wu Y-H 2017 Preliminary dosimetric study on feasibility of multi-beam boron neutron capture therapy in patients with diffuse intrinsic pontine glioma without craniotomy *PLoS One* **12** e0180461

Lee P-Y, Liu Y-H and Jiang S-H 2014 Dosimetric performance evaluation regarding proton beam incident angles of a lithium-based AB-BNCT design *Radiat. Prot. Dosim.* **161** 403–9

Li W, Zhang W, Lin Y, Chen R C and Gao H 2023 Fraction optimization for hybrid proton–photon treatment planning *Med. Phys.* **50** 3311–23

Marc L, Fabiano S, Wahl N, Linsenmeier C, Lomax A J and Unkelbach J 2021 Combined proton–photon treatment for breast cancer *Phys. Med. Biol.* **66** 235002

Paganetti H 2012 Range uncertainties in proton therapy and the role of Monte Carlo simulations *Phys. Med. Biol.* **57** R99

Palmer M R, Goorley J T, Kiger W III, Busse P M, Riley K J, Harling O K and Zamenhof R G 2002 Treatment planning and dosimetry for the Harvard-MIT Phase I clinical trial of cranial neutron capture therapy *Int. J. Radiat. Oncol.* Biol.* Phys.* **53** 1361–79

Perl J, Shin J, Schümann J, Faddegon B and Paganetti H 2012 TOPAS: an innovative proton Monte Carlo platform for research and clinical applications *Med. Phys.* **39** 6818–37

Renaud M A, Serban M and Seuntjens J 2019 Robust mixed electron–photon radiation therapy optimization *Med. Phys.* **46** 1384–96

Reya T, Morrison S J, Clarke M F and Weissman I L 2001 Stem cells, cancer, and cancer stem cells *Nature* **414** 105–11

Sato T, Masunaga S-i, Kumada H and Hamada N 2018 Microdosimetric modeling of biological effectiveness for boron neutron capture therapy considering intra-and intercellular heterogeneity in 10B distribution *Sci. Rep.* **8** 988

Schneider W, Bortfeld T and Schlegel W 2000 Correlation between CT numbers and tissue parameters needed for Monte Carlo simulations of clinical dose distributions *Phys. Med. Biol.* **45** 459

Sharma P and Allison J P 2015 The future of immune checkpoint therapy *Science* **348** 56–61

Takada K, Kumada H, Matsumura A, Sakurai H and Sakae T 2020 Computational evaluation of dose distribution for BNCT treatment combined with x-ray therapy or proton beam therapy *Appl. Radiat. Isot.* **165** 109295

Teng Y-C, Chen J, Zhong W-B and Liu Y-H 2023 Correcting for the heterogeneous boron distribution in a tumor for BNCT dose calculation *Sci. Rep.* **13** 15741

Tsujii H, Mizoe J-e, Kamada T, Baba M, Kato S, Kato H, Tsuji H, Yamada S, Yasuda S and Ohno T 2004 Overview of clinical experiences on carbon ion radiotherapy at NIRS *Radiother. Oncol.* **73** S41–9

Unkelbach J, Bangert M, Bernstein K D A, Andratschke N and Guckenberger M 2018 Optimization of combined proton–photon treatments *Radiother. Oncol.* **128** 133–8

Wieser H P, Cisternas E, Wahl N, Ulrich S, Stadler A, Mescher H, Müller L R, Klinge T, Gabrys H and Burigo L 2017 Development of the open-source dose calculation and optimization toolkit matRad *Med. Phys.* **44** 2556–68

Wilkens J and Oelfke U 2004 A phenomenological model for the relative biological effectiveness in therapeutic proton beams *Phys. Med. Biol.* **49** 2811

Wilkens J J and Oelfke U 2006 Fast multifield optimization of the biological effect in ion therapy *Phys. Med. Biol.* **51** 3127

Wu R-Y, Geng C-R, Tian F, Yao Z-Y, Gong C-H, Han H-N, Xu J-F, Xiao Y-S and Tang X-B 2023 GPU-accelerated three-dimensional reconstruction method of the Compton camera and its application in radionuclide imaging *Nucl. Sci. Tech.* **34** 52

Yu H, Tang X, Shu D, Geng C, Gong C, Hang S and Chen D 2017 Impacts of multiple-field irradiation and boron concentration on the treatment of boron neutron capture therapy for non-small cell lung cancer *Int. J. Radiat. Res.* **15** 1–13 http://ijrr.com/article-1-1881-en.html

Zhang X, Geng C, Tang X, Bortolussi S, Shu D, Gong C, Han Y and Wu S 2019 Assessment of long-term risks of secondary cancer in paediatric patients with brain tumours after boron neutron capture therapy *J. Radiol. Prot.* **39** 838